A COMPUTATIONAL CONSTITUTIVE MODEL FOR CONCRETE SUBJECTED TO LARGE STRAINS, HIGH STRAIN RATES, AND HIGH PRESSURES

mat III

T. J. Holmquist and Dr. G. R. Johnson
Alliant Techsystems Inc.
Hopkins, Minnesota USA

and

Dr. W. H. Cook
Wright Laboratory, Armament Directorate
Eglin Air Force Base, Florida USA

This paper presents a computational constitutive model for concrete subjected to large strains, high strain rates, and high pressures; and is well-suited for computations in both Lagrangian and Eulerian codes. The equivalent strength is expressed as a function of the pressure, strain rate, and damage. The pressure is expressed as a function of the volumetric strain and includes the effect of permanent crushing. The damage is accumulated as a function of the plastic volumetric strain, equivalent plastic strain, and pressure. The cohesive component of the equivalent strength is degraded as the damage accumulates. Constants are determined for 0.048 GPa (7000 psi) unconfined compressive strength concrete, and an example is presented to illustrate the model. Computations are presented for a penetrator impacting a concrete target at various velocities, and the results are compared to test data.

INTRODUCTION

Recently, much effort has been directed at modeling the behavior of concrete for use in computer codes. The majority of this work has been done for relatively small strains, low strain rates, and low pressures, in support of civil engineering applications. Much less work has been directed toward modeling concrete for impact computations where the material experiences large strains, high strain rates, and high pressures.

This paper presents a computational constitutive model for concrete subjected to large strains, high strain rates, and high pressures; and is well-suited for computations in both Lagrangian and Eulerian codes. The model is similar to that developed by Osborn [1], but is expanded to include material damage, strain rate effects, and permanent crushing as a function of the pressure and air void ratio.

The remainder of this paper presents a description of the model, determination of constants for 0.048 GPa (7000 psi) unconfined compressive strength concrete, and penetration computations that are compared to test data.

DESCRIPTION OF THE MODEL

A general overview of the model is presented in Figure 1. The strength portion of the model is shown on the top of Figure 1. The normalized equivalent stress is defined as, $\sigma^* = \sigma/f'_c$, where σ is the actual equivalent stress and $f'c$ is the quasi-static uniaxial compressive strength. The specific expression is

$$\sigma^* = [A(1-D) + BP^{*N}][1 + C\ln\dot{\varepsilon}^*] \qquad (1)$$

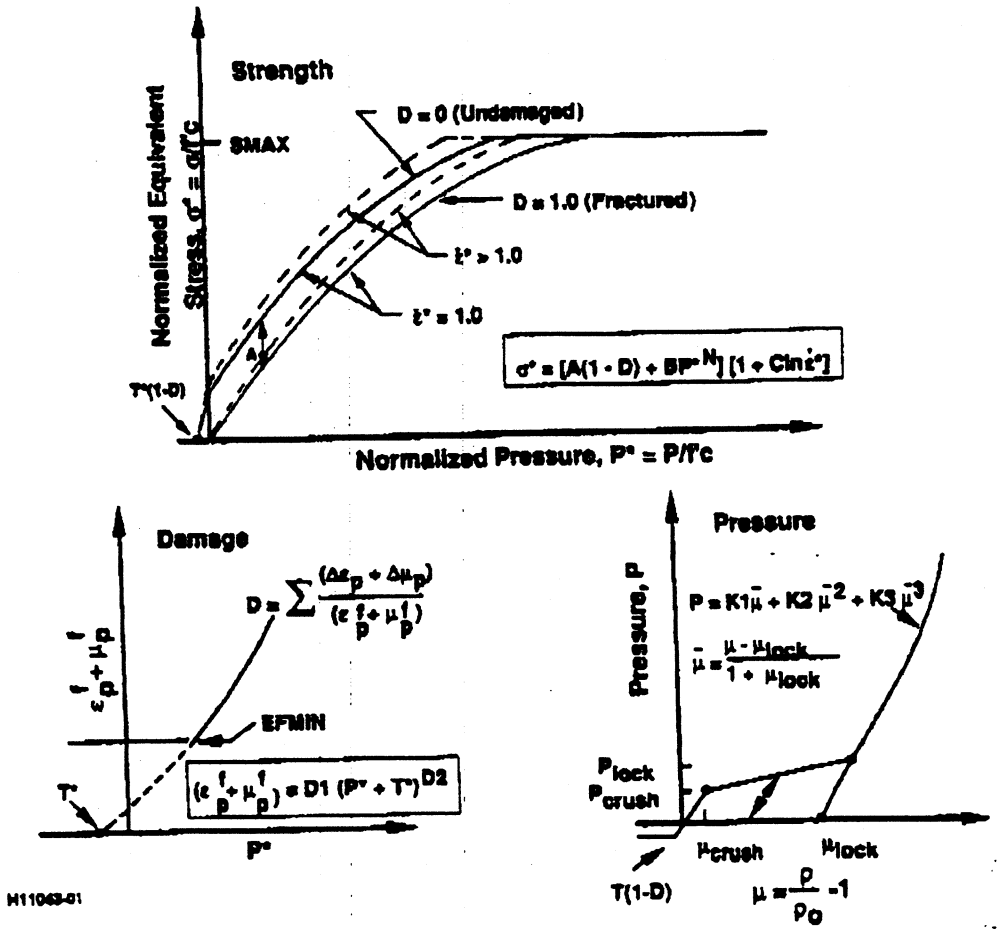

Figure 1. Description of the Model

where D is the damage ($0 \le D \le 1.0$), $P^* = P/f'_c$ is the normalized pressure (where P is the actual pressure), and $\dot{\varepsilon}^* = \dot{\varepsilon}/\dot{\varepsilon}_0$ is the dimensionless strain rate (where $\dot{\varepsilon}$ is the actual strain rate and $\dot{\varepsilon}_0 = 1.0s^{-1}$ is the reference strain rate). The normalized maximum tensile hydrostatic pressure is $T^* = T/f'_c$, where T is the maximum tensile hydrostatic pressure the material can withstand.

The material constants are A, B, N, C and SMAX, where A is the normalized cohesive strength, B is the normalized pressure hardening coefficient, N is the pressure hardening exponent, C is the strain rate coefficient, and SMAX is the normalized maximum strength that can be developed.

The damage for fracture is shown in the lower left corner of Figure 1. It is accumulated in a manner similar to that used in the Johnson-Cook fracture model [2]. The Johnson-Cook fracture model accumulates damage from equivalent plastic strain. The model discussed herein accumulates damage from both equivalent plastic strain and plastic volumetric strain, and is expressed as

$$D = \sum \frac{\Delta\varepsilon_p + \Delta\mu_p}{\varepsilon_p^f + \mu_p^f} \qquad (2)$$

where $\Delta\varepsilon_p$ and $\Delta\mu_p$ are the equivalent plastic strain and plastic volumetric strain, respectively, during a cycle of integration; and $\varepsilon_p^f + \mu_p^f = f(P)$ is the plastic strain to fracture under a constant pressure, P. The specific expression is

$$\varepsilon_p^f + \mu_p^f = D1(P^* + T^*)^{D2} \tag{3}$$

where D1 and D2 are constants and P^* and T^* are as defined previously. As is evident from equation 3, the concrete material cannot undergo any plastic strain at $P^* = -T^*$ and alternatively, the plastic strain to fracture increases as P^* increases. A third damage constant, EFMIN, is provided to allow for a finite amount of plastic strain to fracture the material. This is included to suppress fracture from low magnitude tensile waves.

Damage due to plastic volumetric strain is included in equations 2 and 3 because the concrete will lose cohesive strength during air void collapse. Under most circumstances, the majority of the damage will occur from equivalent plastic strain.

The hydrostatic pressure-volume relationship is presented in the lower right corner of Figure 1. The pressure-volume response is separated into three response regions. The first region is linear elastic and occurs at $P \le P_{crush}$. P_{crush} and μ_{crush} are the pressure and volumetric strain that occur in a uniaxial stress compression test, and T is as previously defined. The elastic bulk modulus is $K_{elastic} = P_{crush} / \mu_{crush}$.

The second region is referred to as the transition region and occurs at $P_{crush} \le P \le P_{lock}$. In this region, the air voids are gradually compressed out of the concrete producing plastic volumetric strain. Unloading in this region occurs along a modified path that is interpolated from the adjacent regions.

The third region defines the relationship for fully dense material (all air voids removed from the concrete). The air voids are completely removed from the material when the pressure reaches P_{lock} and the relationship is expressed as

$$P = K1\bar{\mu} + K2\bar{\mu}^2 + K3\bar{\mu}^3 \tag{4}$$

where

$$\bar{\mu} = \frac{\mu - \mu_{lock}}{1 + \mu_{lock}} \tag{5}$$

The modified volumetric strain, $\bar{\mu}$, is used so that the constants (K1, K2, and K3) are equivalent to those used for material with no voids. The standard volumetric strain is $\mu = \rho/\rho_0 - 1$ for current density ρ and initial density ρ_0. The locking volumetric strain is $\mu_{lock} = \rho_{grain}/\rho_0 - 1$ where ρ_{grain} is the grain density. This is identical to the density of the material with no air voids.

For tensile pressure, $P = K_{elastic} \cdot \mu$ in the elastic region, $P = K1 \cdot \mu$ in the fully dense region, and $P = [(1 - F) \cdot K_{elastic} + F \cdot K1] \cdot \mu$ in the transition region. The interpolation factor is $F = (\mu_{max} - \mu_{crush}) / (\mu_{plock} - \mu_{crush})$ where μ_{max} is the maximum volumetric strain reached prior to unloading and μ_{plock} is the volumetric strain at P_{lock}. A similar method is used for compressive unloading except that the higher order terms ($K2\bar{\mu}^2$ and $K3\bar{\mu}^3$) are included. The tensile pressure is limited to $T(1 - D)$.

DETERMINATION OF CONSTANTS

Figure 2 presents the model characterized for a concrete material having an unconfined compressive strength, $f'_c = 0.048$ GPa (7000 psi). The majority of the test data used to determine the constants was obtained from Hanchak et al. [3], where concrete strength was determined at different confining pressures. Although the constants are consistent with the

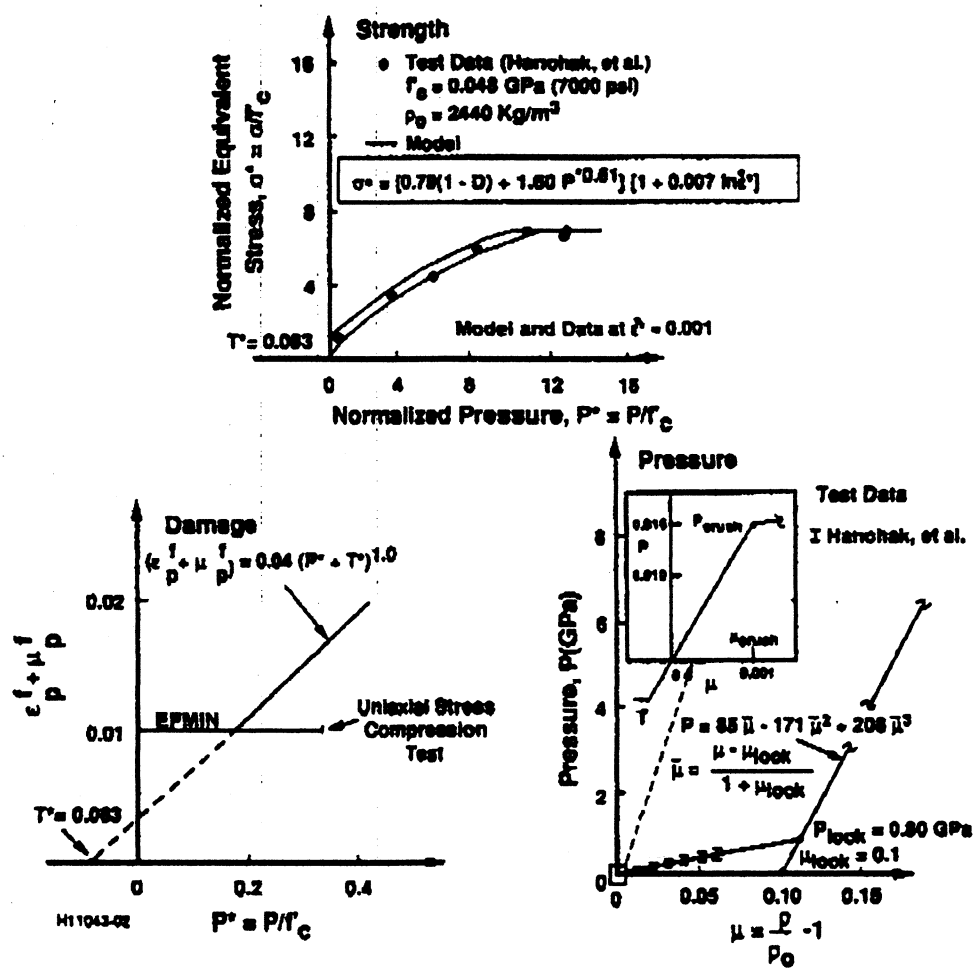

Figure 2. Model Description for f'_c = 0.048 GPa (7000 psi) Concrete

data, in some instances adequate data was not available to explicitly determine each individual constant.

The first step in the process is to determine constants for the strength of the concrete. The constants A, B, N, C, SMAX, and T are required to fully characterize the material strength. The maximum hydrostatic tension, T, is defined as the maximum principle stress in tension the material can support. From the test data in Reference 3, T = 0.004 GPa. Normalizing T by f'_c gives $T^* = 0.083$. The strain rate constant, C, is determined next. Figure 3 shows normalized uniaxial compressive strengths for various concretes as a function of strain rate [4-6]. It is not obvious if the strain rate effect is dependent on the initial concrete strength, f'_c, or if the differences are within experimental error. It will be assumed that rate effects are independent of initial strength and are constant for all concrete. Although the test data in Figure 3 show a substantial strain rate effect, the increase in strength is not solely due to strain rate, but also includes increased pressure effects. This is especially true at higher rates where the stress condition becomes triaxial as opposed to uniaxial. To obtain the strain rate effect alone, the pressure effect must be removed.

Figure 4 presents the technique used to remove the pressure effect and obtain the strain rate constant. On the left side of Figure 4, the normalized uniaxial compressive strengths, for the three strain rates from Figure 3, are shown as a function of normalized pressure, assuming a

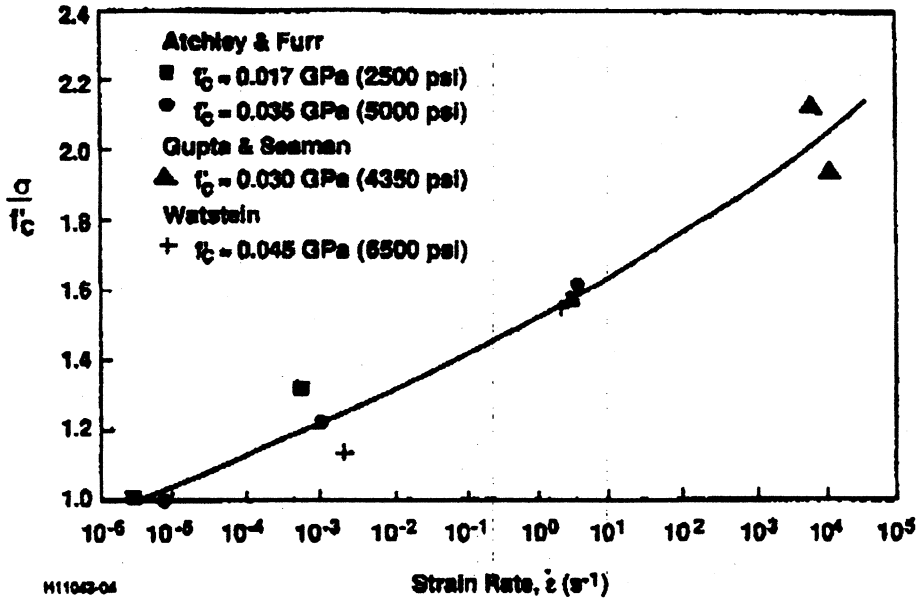

Figure 3. Concrete Strength as a Function of Strain Rate

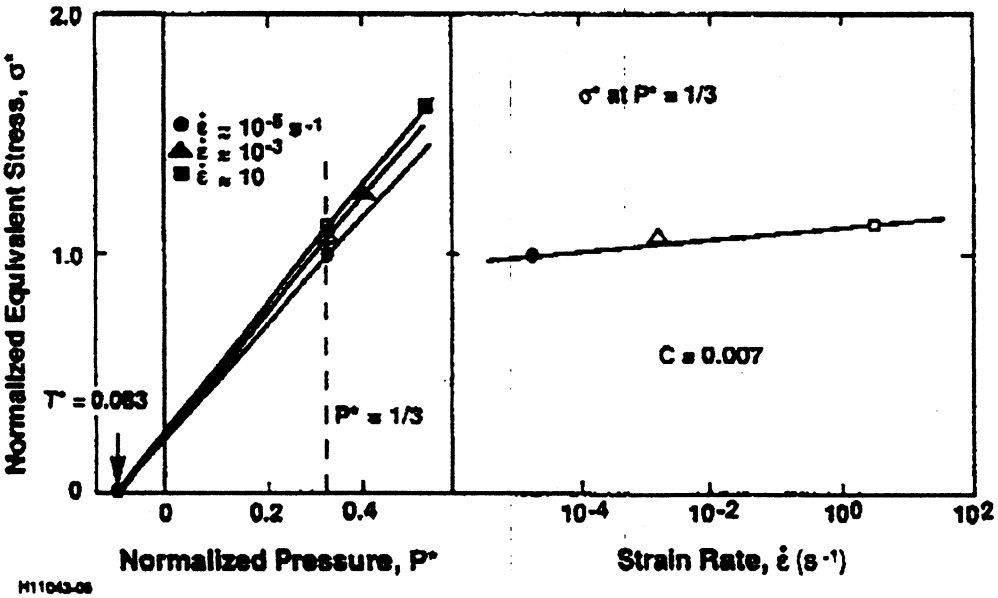

Figure 4. Strain Rate Sensitivity and Constant Determination for Concrete

uniaxial stress condition. The high rate data ($\dot{\varepsilon} \approx 10^4$ s^{-1}) are not used because of the unknown stress state. A straight line is drawn from the maximum normalized hydrostatic pressure, $T^* = 0.083$, through each of the test data. The change in slope between each line provides a measure of the strain rate effect. The change in strength, due to strain rate alone, is determined at a constant normalized pressure, $P^* = 1/3$, corresponding to the data at $\dot{\varepsilon} = 10^{-5}$ s^{-1}. The constant $C = 0.007$ is obtained by performing a least squares fit through the three data points as shown.

The remaining strength constants, A, B, N, and SMAX, are determined using the test data provided by Hanchak et al. [3] and by making some assumptions. The constant, A, defines the

normalize cohesive strength of the material at $\dot{\varepsilon}^* = 1.0$. The cohesive strength is defined as the difference between the undamaged strength and the completely fractured strength at a given pressure. Although the test data provide a general description of the concrete behavior over a wide range of pressures, there are little data at lower pressures ($P^* < 4$) where the cohesive strength of concrete is most apparent. Due to the lack of test data in the area of interest, the cohesive strength will be assumed to be 0.75f'c for quasi-static conditions ($\dot{\varepsilon}^* = 0.001$). Normalizing to $\dot{\varepsilon}^* = 1.0$ gives A = 0.79.

Constants B and N define the normalized fractured material strength at $\dot{\varepsilon}^* = 1.0$. These constants are determined to provide a lower bound for the data. Setting B = 1.60 and N = 0.61 provides a good fit to the data as shown in Figure 2. Lastly, SMAX is determined. The test data indicate that the compressive strength no longer increases with increasing pressure. For these data, SMAX = 7.0. Although there were assumptions made to determine the strength constants due to a lack of test data, the model fits the available test data well.

The damage model constants, D1, D2, and EFMIN, are determined next. Figure 5 shows the stress-strain results for a cylinder subjected to cyclic compression loading [7]. An assumed failure surface is defined from the test results, indicating a total loss in strength at an axial strain of $\varepsilon_x = 0.01$. If the elastic axial strain, ε_{xe}, and volumetric strain, μ, are taken to be zero, the equivalent plastic strain at fracture is $\varepsilon_p^f = 0.01$. The plastic strain occurs over a pressure range from 0 to 1/3f'c. There is some justification for assuming $\varepsilon_{xe} = \mu = 0$ for a uniaxial compression test. The elastic strain is probably small due to the early curvature of the modulus as shown in Figure 5, and the volumetric strain is also probably small due to the low pressures that occur ($P = 1/3\sigma_x$).

The damage model constant, D1, is determined using $T^* = 0.083$ and the equivalent plastic fracture strain, $\varepsilon_p^f = 0.01$, from the uniaxial compression test. D2 is set to 1.0 due to insufficient test data. Initiating the damage curve at $T^* = 0.083$ and satisfying the equivalent plastic fracture strain at $P^* = 1/6$, the constant, D1 = 0.04, is determined. To suppress fracture from low magnitude tensile waves, EFMIN is set to 0.01.

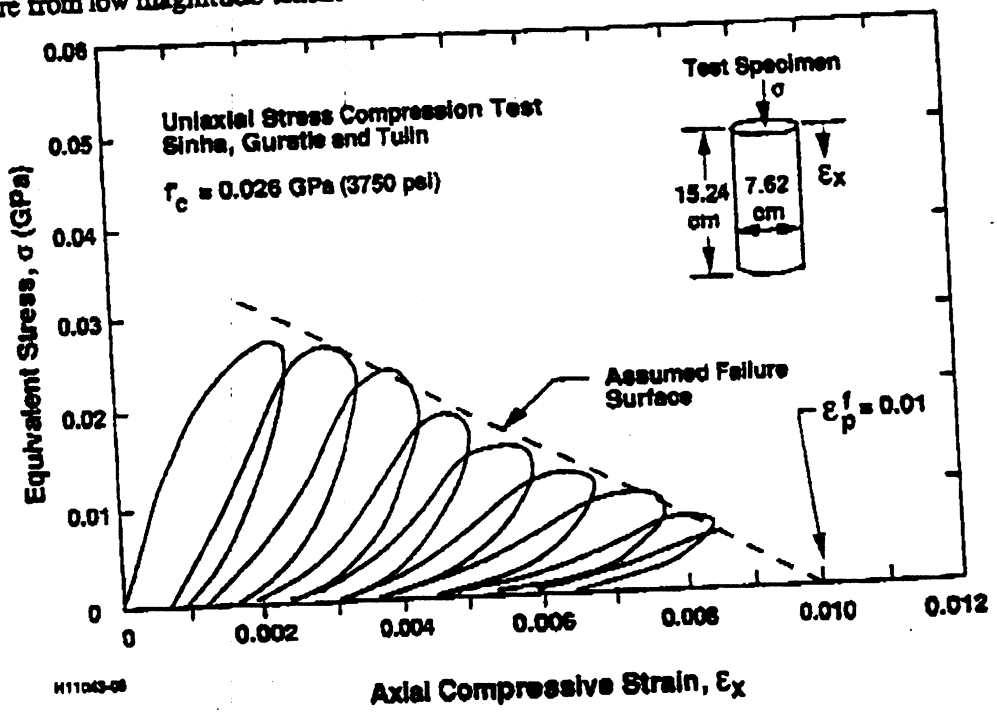

Figure 5. Concrete Softening (damage) Due to Deviator and Shear Strain

Lastly, the pressure constants, P_{crush}, μ_{crush}, P_{lock}, μ_{lock}, K1, K2, and K3, are determined. $P_{crush} = f'c / 3 = 16$ GPa and $\mu_{crush} = P_{crush} / K_{elastic} = 0.001$ where $K_{elastic}$ is determined from elasticity theory using Young's modulus, (E = 35.7 GPa), and Poisson's ratio, ($\nu = 0.2$) [8]. The air void ratio is $\mu_{lock} = \rho_{grain} / \rho_o - 1 = 0.1$, where $\rho_{grain} = 2680$ kg/m^3 [9] and $\rho_o = 2440$ kg/m3. The grain density, ρ_{grain}, was not provided for this concrete. The value used was obtained from Grady [9] where a similar concrete was investigated. The constants for the fully crushed curve are K1 = 85 GPa, K2 = –171 GPa, and K3 = 208 GPa. The constants were obtained from shock Hugoniot data [10] for granite and quartz. The average density for granite and quartz is approximately 2640 kg/m^3, which is consistent with the grain density. $P_{lock} = 0.80$ GPa is the pressure at which all the air voids are removed from the concrete. P_{lock} is determined by providing a best fit to the data as shown in Figure 2.

All the constants for a concrete material having an unconfined compressive strength, $f'c = 0.048$ GPa (7000 psi), have been defined and are summarized in Table 1. An example of how the model behaves, using these constants, is provided in Figure 6. A quasi-static, uniaxial strain compression test is simulated to illustrate the model. The material behaves essentially elastic from point 1 to point 2, although there is a small amount of plastic volumetric strain that occurs. At point 2, the yield surface is reached and equivalent plastic strain begins to accumulate. From point 2 to point 3, the increase in equivalent plastic strain causes the material to damage, which in turn causes a gradual loss in cohesive strength. At point 3, the maximum strength is reached and the material continues to flow plastically and accumulate damage until the loading is reversed at point 4. From point 4 to point 5, the unloading is elastic. The yield surface is again encountered at point 5 and the material continues to flow plastically until the load is removed at point 6. Of special interest is the elastic unloading response between points 4 and 5. The unloading path is different than the elastic loading that occurs between points 1 and 2 due to the crushing of the material.

Table 1. Summary of Constants for $f'_c = 0.048$ GPa (7000 psi) Concrete

Mass/Thermal Constants		
Density	(Kg/m^3)	2440
Specific Heat	(J/Kg • K)	654
Strength Constants		
A		0.79
B		1.60
N		0.61
C		0.007
f'_c	(GPa)	0.048
SMAX		7.0
Shear Modulus	(GPa)	14.86
Damage Constants		
D1		0.04
D2		1.0
EFMIN		0.01
Pressure Constants		
P_{crush}	(GPa)	0.016
μ_{crush}		0.001
K1	(GPa)	85
K2	(GPa)	-171
K3	(GPa)	208
P_{lock}	(GPa)	0.80
μ_{lock}		0.10
T	(GPa)	0.004

NT1210-08

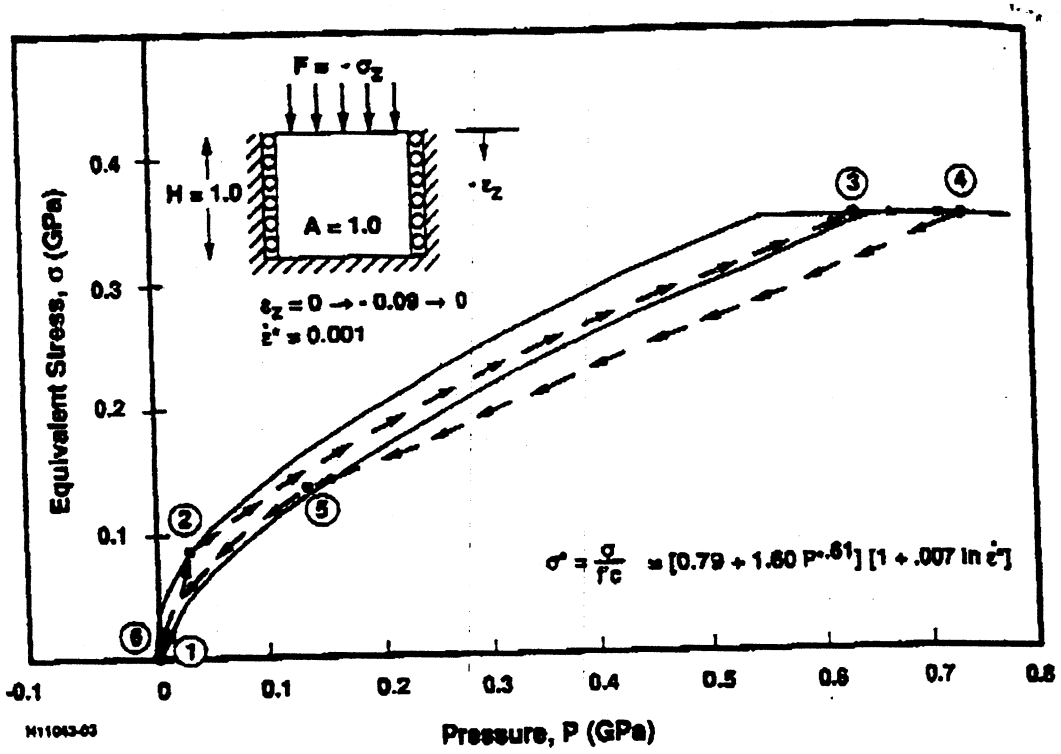

Figure 6. Example Using the Model

PENETRATION COMPUTATIONS AND COMPARISON TO TEST DATA

Penetration computations of tests performed by Hanchak, et al., [3] were performed to demonstrate and verify the model. A description of the problem, including results at various computational times, is provided in Figure 7 for an impact velocity of 400 m/s. Figure 8 shows the impact velocity verses residual velocity for the experimental and computational results. The computed results show good general agreement with the experimental results. The results from the computations used the model and constants determined in the previous section. There was no rebar in the computations, although the tested concrete did have rebar. Some approximate computations with rebar indicated that it had little effect in the residual velocity. The effect of friction, however, does have an effect, especially at lower velocities.

SUMMARY AND CONCLUSIONS

A computational constitutive model has been presented for concrete material subjected to large strains, high strain rates, and high pressures. Constants were determined for the model using test data for f'c = 0.048 GPa (7000 psi) compressive strength concrete, and an example was presented to illustrate the behavior. A series of two-dimensional computations were performed using the model, and the results were compared to experimental data. The computational results compared reasonably well to the experiments, although additional concrete test data are required to allow all of the constants to be obtained in an explicit manner.

ACKNOWLEDGMENTS

This work was funded by Contract F08630-92-C-0006 from Wright Laboratory, Armament Directorate, Eglin Air Force Base.

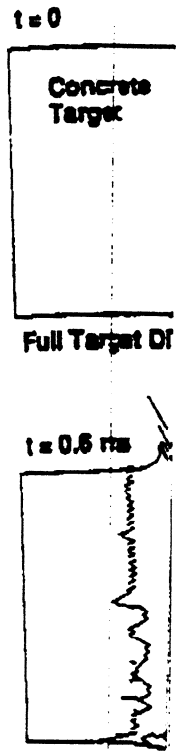

Figure 7.

REFERENCES

[1] D. A. Mat
Dimension
July 1982.

[2] G. R. Johns
Various St
Fracture M

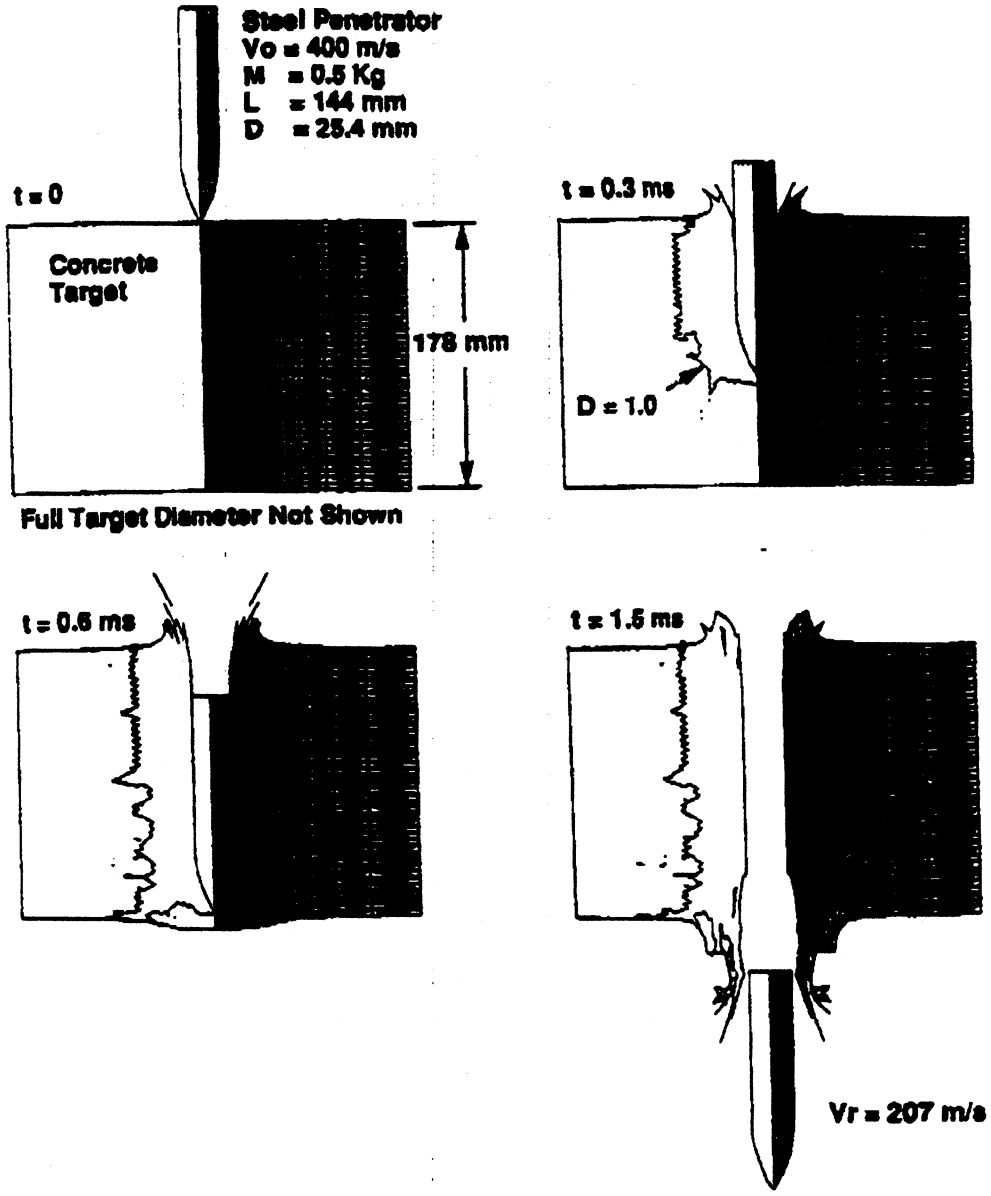

Figure 7. Penetration Results at Various Times of the Computation

REFERENCES

[1] D. A. Matuska, R. E. Durrett, and J. J. Osborn, "Hull Users Guide for Three-Dimensional Linking with EPIC 3," ARBRL-CR-00484, Orlando Technology Inc., July 1982.

[2] G. R. Johnson and W. H. Cook, "Fracture Characteristics of Three Metals Subjected to Various Strains, Strain Rates, Temperatures and Pressures," *Journal of Engineering Fracture Mechanics*, Vol. 21, No. 1, pp. 31-48, 1985.

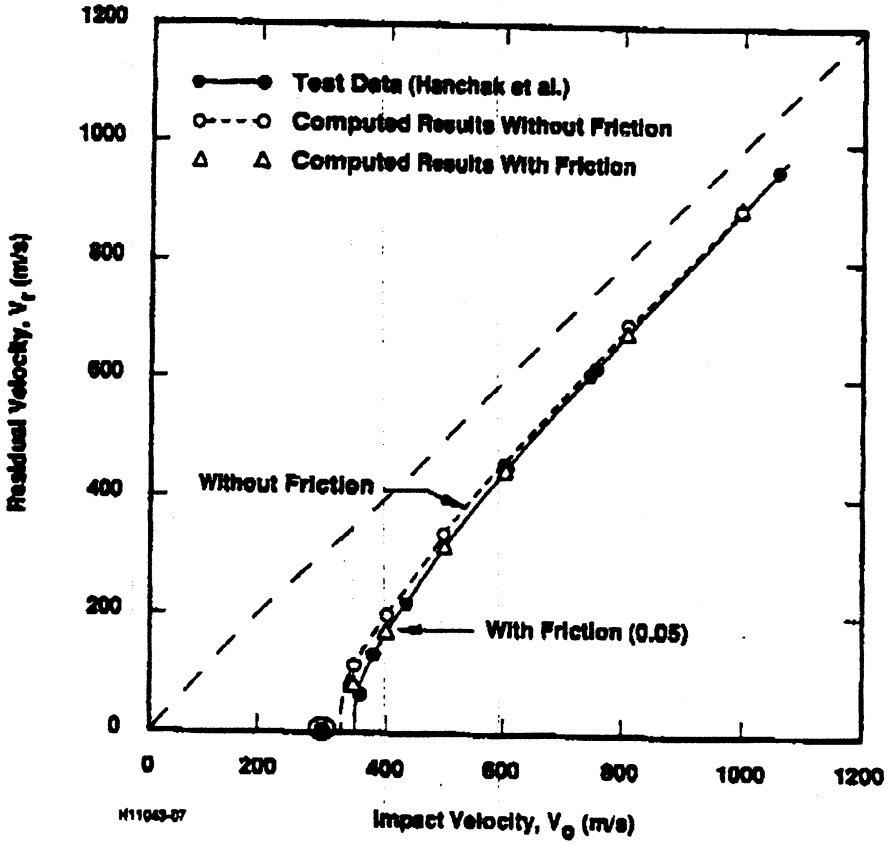

Figure 8. Impact Velocity Versus Residual Velocity for Test Data and Computational Results

[3] S. J. Hanchak, M. J. Forrestal, E. R. Young, and J. Q. Ehrgott, "Perforation of Concrete Slabs with 48 MPa (7 ksi) and 140 MPa (20 ksi) Unconfined Compressive Strengths," *International Journal of Impact Engineering*, Vol. 12, No. 1, pp. 1-7, 1992.

[4] B. L. Atchley and J. H. Furr, "Strength and Energy Absorption Capabilities of Plain Concrete Under Dynamic and Static Loadings," *Journal of the American Concrete Institute*, pp. 745, November, 1967.

[5] Y. M. Gupta and L. Seaman, "Local Response of Reinforced Concrete to Missile Impact," Report NP-1217. SRI International, Menlo Park, CA, October, 1979.

[6] D. Watstein, "Effect of Straining Rate on the Compressive Strength and Elastic Properties of Concrete," *Journal of the American Concrete Institute*, pp. 729, April, 1953.

[7] B. P. Sinha, K. H. Gerstle, and L. G. Tulin, "Stress-Strain Relations for Concrete under Cyclic Loading," *Journal of the American Concrete Institute*, 61 (2), pp. 195-210, February, 1964.

[8] C. Wang and C. G. Salmon, "*Reinforced Concrete Design*, 3rd edition," Harper and Row, New York, 1979.

[9] D. E. Grady, "Impact Compression Properties of Concrete," *Proceedings of the Sixth International Symposium on Interaction of Non nuclear Munitions with Structures*, Panama City Florida, May, 1993.

[10] S. P. Marsh, "LASL Shock Hugoniot Data," University of California Press, 1980.